



# Mineralocorticoid receptor excessive activation involved in glucocorticoid-related brain injury

Yaxi Chen, Yerong Yu\*, Jingtao Qiao, Leilei Zhu, Zhen Xiao

Department of Endocrinology and Metabolism, West China Hospital, Sichuan University, Chengdu, Sichuan, China

## ARTICLE INFO

### Keywords:

Mineralocorticoid receptor  
Hydrocortisone  
Spironolactone  
Cortex  
Hippocampus  
Cerebral artery

## ABSTRACT

The mechanisms involved in brain damage during chronic glucocorticoid exposure are poorly understood. Since mineralocorticoid receptor (MR) activation has been proven to be important in the pathophysiology of vascular damage and MRs are highly expressed in many brain regions, we hypothesized that the cerebral injury observed in subjects with Cushing syndrome is in part associated with the overactivation of MR. The aim of this study was to determine whether the cerebral injury observed in chronic hyperglucocorticoidemia animal models is related to excessive MR activation. Male SD rats were divided into five groups: vehicle, hydrocortisone (HC, 5 mg/kg/day, i.g.), HC + spironolactone (SL, 20 mg/kg/d in chow), dexamethasone (DXM, 0.25 mg/kg/day, i.g.), and DXM + SL (20 mg/kg/d in chow). Compared to the vehicle-treated group, HC-treated rats had higher blood pressure and higher levels of cerebral vascular fibrosis, cortical/hippocampal atrophy, reactive oxygen species (ROS) production and proinflammatory gene expression. However, in HC-treated animals, treatment with SL markedly alleviated ROS production, cerebral and cerebrovascular morphological changes and inflammation but failed to reduce blood pressure. In contrast, DXM induced no cerebral morphological changes except fibrosis in cerebral vessels, an effect that was not ameliorated by SL treatment. These findings demonstrate that the excessive MR activation observed following chronic hyperglucocorticoidemia exposure contributes to cerebrovascular fibrosis and remodeling and promotes neural apoptosis in the cerebral cortex/hippocampus.

## 1. Introduction

Patients with Cushing's syndrome are characterized by chronic hypercortisolism and have been reported to exhibit brain atrophy and related functional alterations [1]. The neurotoxic effects of excess corticosteroids on the brain have also been reported in experimental animals [2,3]. However, the exact mechanisms underlying the brain damage observed during chronic glucocorticoid exposure are poorly understood.

The biological effects of glucocorticoids are mediated in a complementary manner by mineralocorticoid receptors (MRs) and glucocorticoid receptors (GRs) [4]. The affinities of aldosterone and glucocorticoids (cortisol in humans and corticosterone in rodents) for MRs are similar [5]. The plasma concentration of glucocorticoids is 1000

times greater than that of aldosterone under physiological conditions [6,7]. Ligand selectivity for MRs is maintained by 11 $\beta$ -hydroxysteroid dehydrogenase type 2 (11 $\beta$ -HSD2), which transforms glucocorticoids into inactive metabolites, thus preventing the activation of MRs by glucocorticoids [8].

In some cell types, including cardiomyocytes, 11 $\beta$ HSD2 is absent, allowing cortisol to bind to MR and regulate its activities [9]. Rafiq et al. reported that chronic glucocorticoid excess could activate MR and induce the development of renal injury [10]. 11 $\beta$ -HSD1 is widely distributed throughout the brain, while 11 $\beta$ -HSD2 is only in scattered specific cells of the brain [11]. In Cushing's syndrome, the saturation of 11-HSD2 causes MR overactivation in renal epithelial tissues, resulting in an expansion in volume due to sodium retention [12]. Accumulating evidence indicates that MR activation plays an important

**Abbreviations:** 11 $\beta$ -HSD, 11 $\beta$ -hydroxysteroid dehydrogenase; ANOVA, analysis of variance; CCL, C-C motif ligand; CCR2, C-C motif chemokine receptor type 2; DAPI, 4',6-diamidino-2-phenylindole; eNOS, endothelial nitric oxide synthetase; GAPDH, glyceraldehyde-3-phosphate dehydrogenase; GR, glucocorticoid receptor; iNOS, inducible nitric oxide synthase; IL-6, interleukin 6; MR, mineralocorticoid receptor; NHE-1, Na<sup>+</sup>/H<sup>+</sup> + exchanger isoform-1; nNOS, neuronal nitric oxide synthase; PBS, phosphate-buffered saline; PCNA, proliferating cell nuclear antigen; ROS, reactive oxygen species; SBP, systolic blood pressure; Sgk-1, serum and glucocorticoid regulated kinases-1; TNF- $\alpha$ , tumor necrosis factor alpha; TUNEL, terminal deoxynucleotidyl transferase dUTP nick end labeling; UACR, urinary albumin-creatinine ratio

\* Corresponding author at: Department of Endocrinology and Metabolism, West China Hospital, Sichuan University, No. 37 Guoxue Xiang, Chengdu, PR China.

E-mail address: [yerongyu@scu.edu.cn](mailto:yerongyu@scu.edu.cn) (Y. Yu).

<https://doi.org/10.1016/j.bioph.2019.109695>

Received 28 September 2019; Received in revised form 15 November 2019; Accepted 22 November 2019

0753-3322/© 2019 The Author(s). Published by Elsevier Masson SAS. This is an open access article under the CC BY-NC-ND license (<http://creativecommons.org/licenses/by-nc-nd/4.0/>).

**Table 1**  
Biological parameters of animals under different treatment.

	Control (n = 16)	HC (n = 16)	HC + SL (n = 14)	DXM (n = 12)	DXM + SL (n = 12)
Body weight before intervention (g)	268.5 ± 5.2	260.0 ± 5.5	262.1 ± 4.4	266.9 ± 4.9	262.5 ± 5.8
Body weight after intervention (g)	538.2 ± 10.8	507.2 ± 6.5**	475.7 ± 4.5##	399.4 ± 2.6**	417.9 ± 4.7**
SBP before intervention (mmHg)	111.4 ± 2.3	113.5 ± 2.8	112.3 ± 2.1	114.9 ± 2.3	115.1 ± 1.7
SBP after intervention (mmHg)	131.7 ± 1.5	150.4 ± 2.0**	149.1 ± 2.0	146.1 ± 2.4**	143.7 ± 2.0**
UACR before intervention (mg/g Cr)	0.92 ± 0.17	0.89 ± 0.22	1.21 ± 0.42	1.06 ± 0.18	1.24 ± 0.25
UACR after intervention (mg/g Cr)	2.03 ± 0.20	8.70 ± 0.41**	4.16 ± 0.41##	5.90 ± 0.45**	5.18 ± 0.41**
Plasma aldosterone concentration (pg/ml)	219.6 ± 24.6	234.8 ± 17.5	251.9 ± 20.9	Not measure	Not measure
Brain weight/body weight (mg/g)	5.21 ± 0.11	4.89 ± 0.09*	5.10 ± 0.08	5.27 ± 0.07	5.13 ± 0.09

**Footnote:** \* $P < 0.05$  \*\* $P < 0.01$  vs. Control. ## $P < 0.05$  ### $P < 0.01$  vs HC group. Values were expressed as mean ± SEM, n = 12-16. SBP: systolic blood pressure; UACR: urinary albumin-to-creatinine ratio.

role in the pathophysiology of vascular damage in the heart and kidneys. A chronically elevated level of aldosterone is an independent cardiovascular risk factor that is associated with an increased risk of stroke [13]. Endothelial cell MRs contribute to cardiac inflammation and artery endothelial dysfunction [14]. Elevated plasma aldosterone levels lead to MR activation and are strongly associated with hypertension, chronic kidney disease, obesity and metabolic syndrome [15].

MRs are highly expressed in many brain tissues [4] and cerebral vessels [16], and chronic administration of aldosterone causes enhanced oxidative stress and endothelial dysfunction in the cerebral circulation [17]. We hypothesized that the cerebral injury observed in subjects with Cushing syndrome is in part associated with the over-activation of MR. Therefore, the aim of this study was to examine whether the cerebral injury observed in subjects with Cushing syndrome is related, at least in part, to the overactivation of MR by hypercortisolemia. We evaluated the morphological changes observed in SD rat brains after administration of hydrocortisone (HC) or dexamethasone (DXM), a glucocorticoid with no apparent MR agonistic activity. The MR antagonist spironolactone (SL) was administered to rats with hyperglucocorticoidemia to clarify the effects of blocking MR activity. Finally, the possible pathophysiological link between brain injury and chronic exposure to elevated glucocorticoids was examined.

## 2. Materials and methods

### 2.1. Animals

Adult male SD rats weighing 180–200 g (Dashuo, Chengdu, China) were housed in an animal facility with a 12-h dark/light cycle and controlled temperature and humidity. Food and water were given ad libitum throughout the study. Animal studies were approved by the Institutional Animal Care and Use Committee of The West China Hospital. The Guide for the Care and Use of Laboratory Animals, eighth edition (2011) (<http://grants.nih.gov/grants/olaw/guide-for-the-care-and-use-of-laboratory-animals.pdf>), was followed.

### 2.2. Experimental procedure

The rats were randomized into five groups of 28 animals each and were treated for 12 weeks as follows: the control group (CON) received 2 ml of normal saline via gavage twice daily; the HC group received HC via gavage (5 mg/kg/d dissolved in NS, 2 ml twice daily); the HC + SL group received the same dose of HC plus SL (Sigma, Germany, 20 mg/kg/d mixed with chow); the DXM group received DXM via gavage (0.25 mg/kg/d, dissolved in NS, 2 ml twice daily); and the DXM + SL group received the same dose of DXM plus SL (20 mg/kg/d). The doses of HC, DXM and SL were determined on the basis of results from previous studies performed in rats [10]. Systolic blood pressure (SBP) was measured in the tails of the animals using a blood pressure recorder (Techman, Chengdu, China) during treatment weeks 0, 4, 8, and 12.

The animals were adapted to the blood pressure recording for at least 5 days before starting the experiments. Urine samples were collected during treatment weeks 0, 4, 8, and 12 using metabolic cages and stored at  $-20^{\circ}\text{C}$  for urinary creatinine and albumin analysis by a diagnostic ELISA kit (JiangLai, Shanghai, China). After the last treatment, the animals were anesthetized with 50 mg/kg pentobarbital and then sacrificed. Blood was collected through the abdominal aorta, and the serum aldosterone concentrations were measured using diagnostic kits (Y-J Biological, Shanghai, China). The left brain was immediately harvested, and the cortex, hippocampus, and cerebral vasculature were separated. Each brain was snap-frozen in liquid nitrogen and then stored at  $-80^{\circ}\text{C}$  for further RNA and protein extraction. The right brain was fixed in 10 % neutral-buffered formalin for histological studies.

### 2.3. RNA extraction and real-time RT-PCR

Total RNA was extracted from rat tissues using TRIzol reagent (Invitrogen, Netherlands). RNA was quantified using a Nanodrop1000D spectrophotometer (Thermo Scientific, America). cDNA synthesis was carried out using a reverse transcription kit (Takara, Japan). mRNA expression levels were determined using TaqMan real-time PCR on a Light-Cycler 96 system with SYBR Green Master Mix (Bio-Rad, America). Changes in gene expression were analyzed using the comparative CT method and normalized to GAPDH expression [18]. The primer sequences used to measure the mRNA expression levels of MR, GR, 11bHSD1, 11bHSD2, serum/glucocorticoid regulated kinase 1 (Sgk-1), Na<sup>+</sup>/H<sup>+</sup> exchanger isoform-1 (NHE-1), endothelial nitric oxide synthetase (eNOS), neuronal nitric oxide synthase (nNOS), pro-fibrotic factors (alpha-smooth muscle actin (a-SMA), type 1 collagen) and proinflammatory markers (C-C motif chemokine receptor 2 (CCR2), C-C motif chemokine ligand (CCL)7, CCL8, CCL12, interleukin (IL)-6, IL-1 $\beta$ , and tumor necrosis factor alpha (TNF- $\alpha$ )) are listed in Supplementary Table 1. All mRNA fold-changes found in each group are expressed in a heat map.

### 2.4. Histology

The rats were perfused with 0.9 % saline solution followed by 4 % phosphate-buffered paraformaldehyde. Afterwards, the brains were removed, postfixed, equilibrated in 30 % sucrose in phosphate-buffered saline (PBS) and embedded in paraffin, then sectioned into 5  $\mu\text{m}$  slices as previously described. Hematoxylin and eosin (H&E) staining and Nissl staining were performed for morphological analysis [19]. Determinations of the vascular wall thickness and the lumen area/wall area ratio of the basilar artery were performed as described previously [20]. The fibrotic area was evaluated by Masson's trichrome staining as described previously. All histological results were observed using a Leica DM 4000B microscope and analyzed using Image-Pro Plus 6.0 software.

## 2.5. Immunohistochemistry

To evaluate apoptosis in the cerebral cortex, hippocampus and middle-large cerebral artery, a terminal deoxynucleotidyl transferase dUTP nick end labeling (TUNEL) assay kit (Roche, German) was used according to the manufacturer's instructions. This labeled apoptotic cells in green, and nuclei were stained blue with DAPI (Cell Signaling Technology, America). Apoptosis is expressed as the ratio of apoptotic cells to total cells. To evaluate microvascular proliferation, large arteries that were positively labelled for  $\alpha$ -smooth muscle actin were excluded. The sections were stained with a CD34 antibody, incubated with a proliferating cell nuclear antigen (PCNA) antibody, and counterstained with DAPI [21]. Endothelial cells were defined as CD34-positive cells. The proliferative rate of endothelial cells is expressed as the number of PCNA-positive endothelial cell nuclei divided by the total number of endothelial cell nuclei [22]. All immunofluorescence staining was assessed and photographed using a Leica DM 4000B microscope. Positive cells were counted using Image-Pro Plus 6.0. All measurements were calculated by analyzing tissues from at least 6 rats in each treatment group.

## 2.6. Intracellular ROS accumulation

Tissues including the cerebral cortex, hippocampus, and brain vessels (the basilar artery, middle cerebral artery and circle of Willis) were rinsed in ice-cold PBS, cut with medical scissors, and homogenized by a glass homogenizer on ice. The homogenate was centrifuged at 10,000 g at 4 °C for 10 min, and the supernatants were collected for ROS detection as previously described [23]. ROS levels were measured using the dichlorofluorescein diacetate (DCF-DA) method with a standard detection kit (Beyotime, China). Then, the distribution of DCF fluorescence was recorded by a fluorospectrophotometer (Thermo, America) at an excitation wavelength of 485 nm and an emission wavelength of 520 nm. All readings were corrected for background. We used the ROS level of the control group as the standard, and the ROS levels in the other groups are expressed as a percentage of the control group.

## 2.7. Statistical analysis

Statistical analyses were performed with SPSS v.19.0 software. All data are expressed as the mean  $\pm$  standard error of the mean. Statistical comparisons of differences were performed using one-way analysis of variance combined with the Newman Keuls post hoc test. P values below 0.05 were considered statistically significant.

## 2.8. Study approval

Animal studies were approved by the Institutional Animal Care and Use Committee of The West China Hospital.

## 3. Results

### 3.1. Biological parameters

Plasma aldosterone concentrations were almost identical among the HC, HC + SL and control groups. During the 12-week treatment period, the rats in the HC group showed less body weight gain than was observed in the control rats, and this phenomenon was more obvious in the HC + SL group (Fig. 1A). HC increased blood pressure, while SL failed to attenuate this change (Fig. 1B). The urinary albumin-creatinine ratio (UACR) was significantly higher in the HC group than in the control group, and SL treatment alleviated renal injury in HC-treated animals (Fig. 1C). Body weight was significantly lower and SBP and UACR higher in both the DXM and DXM + SL groups than in the control group. However, SL treatment did not have any influence on body weight, SBP and UACR of DXM-treated animals (Fig. 1D, E, F). The ratio

of brain weight to body weight was lower in the HC group than in the control group, but this ratio was similar between each of the other groups and the control group (Table 1).

### 3.2. Pathologic morphological changes in the cerebral cortex and hippocampus

The neuronal morphology of the rat brain was observed following HE and Nissl staining. The cortical and hippocampal neurons in the control, DXM and DXM + SL groups were arranged regularly and contained round, large and regular nuclei on HE staining. In the HC group, a considerable number of cells were arranged in a disorderly manner and contained pyknotic or severely shrunken nuclei (Fig. 2A, B). On Nissl staining which was used to identify the neuronal structure, the neurons of the HC rats showed an irregular arrangement, contained hypochromic nuclei and were fewer in number. Compared with the HC group, less cellular damage was observed in the HC + SL group (Fig. 2C, D). TUNEL staining was used to detect cellular apoptosis in the brain. Apoptotic cells were stained green, as shown in Fig. 3A, B. Compared with the control, following HC treatment, the apoptosis rate in the brain was significantly higher, whereas compared with the HC group, in the HC + SL group, the apoptosis rate was significantly lower. Consistent with findings following HE and Nissl staining, there were no clearly apoptotic cells in the DXM and DXM + SL groups (Fig. 3C, D). These analyses show that HC can cause brain injury, and SL partially blocks the toxic effects of HC on the brain.

### 3.3. Pathologic morphological changes in the cerebral artery

We next determined the effects of HC on basilar arterial wall thickening by measuring the inside and outside diameters of arteries. The thicknesses of arterial walls were markedly higher in the HC group than in the control group, an effect that was partially reduced by SL. DXM increased arterial wall thickness to essentially the same thickness observed in the DXM + SL group (Fig. 4 row A, E). In the HC group, the basilar artery wall area was higher while its lumen area was lower, resulting in a higher wall area/lumen area ratio than that was found in the control group, and this effect was reversed by SL treatment. Interestingly, inconsistent with the results obtained for wall thickening, the basilar artery wall area and lumen area were higher in the DXM and DXM + SL groups, in which the wall/lumen area ratio was not different from that observed in the control group (Fig. 4F). We evaluated the fibrotic state of vessels based on the posterior communicating artery (PCoA) and arterioles among the cortex using Masson's trichrome staining, which shows collagen in blue and smooth muscle cells in red. The results showed that vessel wall thickening and the amount of collagen were higher in the HC group than in the control group, whereas the fibrotic area was smaller in the HC + SL group than in the HC group. Moreover, there was more collagen in the DXM and DXM + SL groups than in the control group (Fig. 4 rows B and C).

Additionally, TUNEL staining was used to detect cellular apoptosis in the basilar artery. The apoptosis rate in the basilar artery was significantly higher following HC treatment than in the control group. Compared with the HC group, in the HC + SL group, the apoptosis rate was significantly lower. The DXM and DXM + SL groups also showed clearly apoptotic cells (Fig. 4 row D, G). These analyses show that HC can cause cerebral vascular injury and that SL partially blocks the toxic effects of HC on vessels.

### 3.4. Microvascular changes in the cortex and hippocampus

To evaluate microvascular changes in the cortex and hippocampus, we costained tissues for PCNA or CD34 (a microvascular endothelial marker) (each is shown in red) and DAPI (nuclear marker, shown in blue). The proliferation of endothelial cells was quantified using PCNA positivity in endothelial cell nuclei as an index. Immunofluorescence

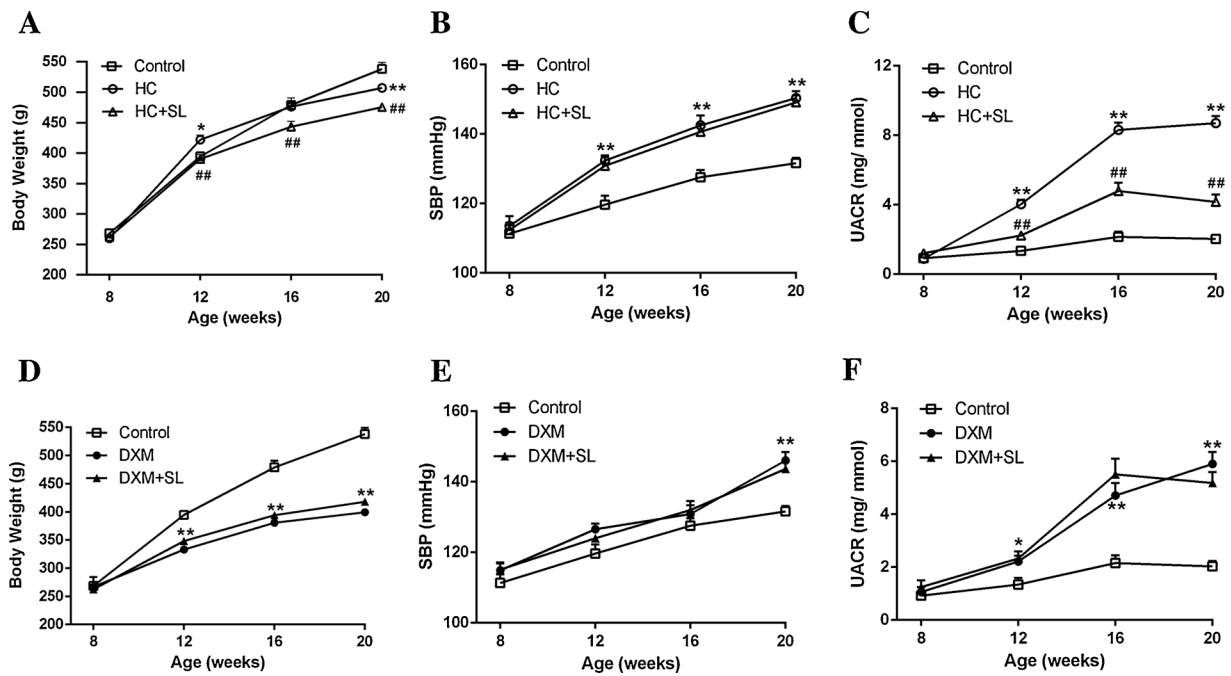


Fig. 1. Body weight, SBP and UACR of animals under different treatment.

Both HC and DXM animals developed decreased body weight (A and D), increased hypertension (B and E), and albuminuria (C and F). Spironolactone affect neither HC nor DXM-induced SBP elevation, but markedly ameliorated albuminuria in HC-treated rats but not in DXM-rats. \*P < 0.05 \*\*P < 0.01 vs. Control. #P < 0.05 ##P < 0.01 vs HC group. Values were expressed as mean ± SEM, n = 12-16. SBP: systolic blood pressure; UACR: urinary albumin-to-creatinine ratio.

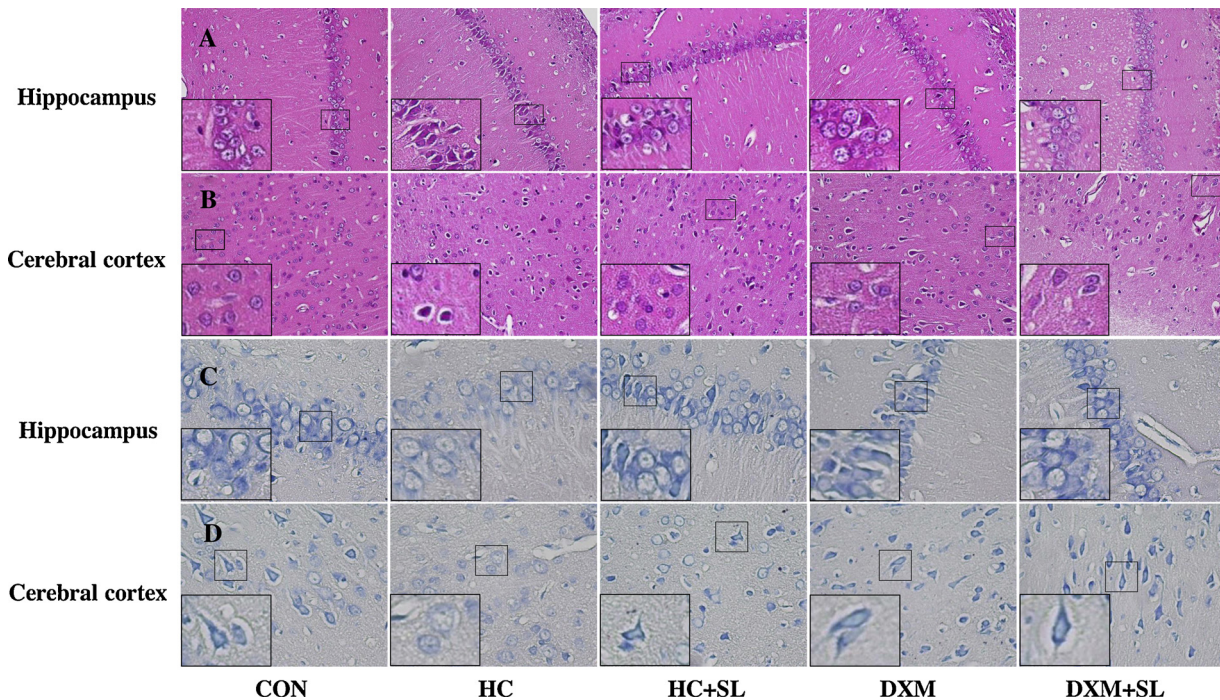


Fig. 2. The neuronal morphology in different groups (magnification: A, B: ×200, C, D: ×400).

DXM and DXM + SL groups were arranged regularly with round, large and regular nuclei by HE and Nissl staining. In the HC treatment, neurons were arranged disorderly, with pyknotic or severely shrunken nuclei (Row A, B) and showed irregular arrangement with hypochromic nuclei by Nissl staining (Row C, D). Compared with the HC group, less cellular damage was observed in the HC + SL group. The featured cells were indicated by squares. n = 6 for each experiment.

staining showed that compared to the control group, in the HC group, microvascular proliferation was significantly inhibited. Finally, the administration of SL caused the number of proliferative cells to increase in both the cortex and the hippocampus (Fig. 5, detailed in Supplemental Figs. 1,2).

### 3.5. ROS levels in the cerebral artery, cerebral cortex and hippocampus

Compare to the control group, in the HC group, the ROS levels in the cerebral artery, cerebral cortex and hippocampus increased by 93.3 % (P < 0.05 vs. CON), 158 % (P < 0.05 vs. CON) and 221% (P < 0.05 vs. CON), respectively. Spironolactone partially reversed these changes,

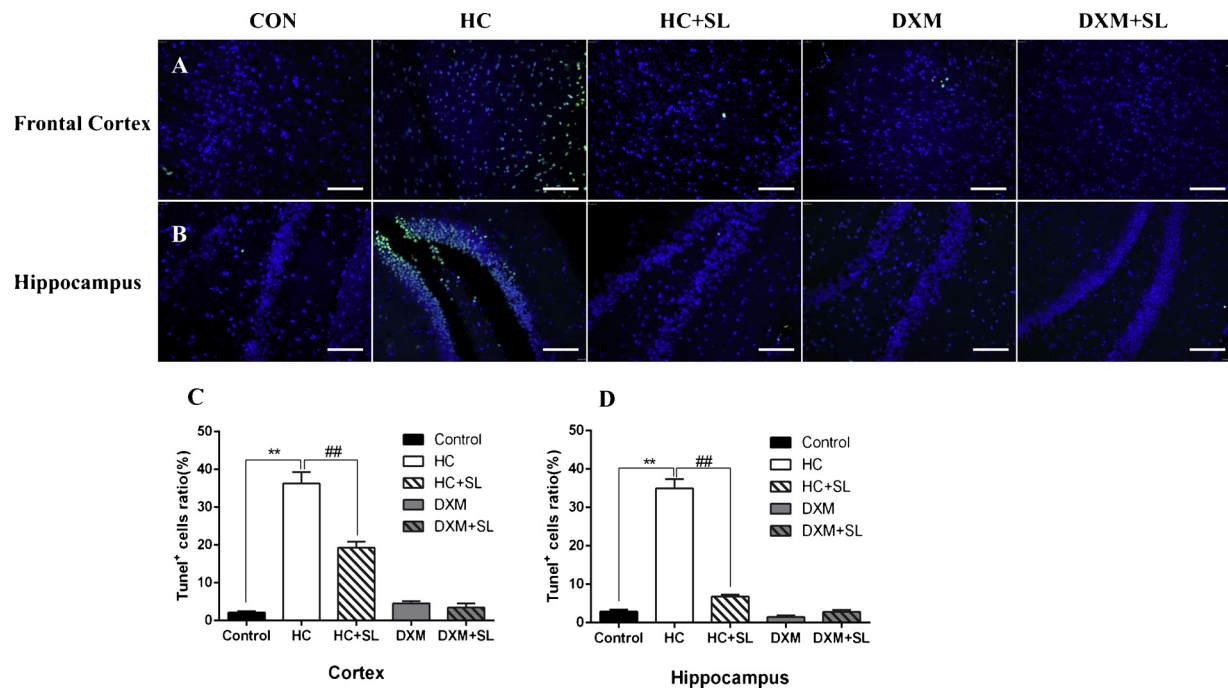


**Fig. 3.** Apoptosis in cerebral cortex and hippocampus (magnification: A, B:  $\times 200$ ).

Photomicrographs of the cortex (Row A) and hippocampus (Row B) for the TUNEL assay. The apoptosis cells were stained in green; Quantification of apoptotic cells by the TUNEL assay (C and D) was significantly increased following HC treatment and can be reversed by spironolactone. Apoptosis was expressed as the ratio of apoptotic cells to total cells (nuclei stained in blue). The data are expressed as mean  $\pm$  SEM.  $n = 6$ . \* $P < 0.05$  \*\* $P < 0.01$  vs Control. # $P < 0.05$  ## $P < 0.01$  vs HC group. Scale bars = 50  $\mu\text{m}$ .

and the ROS levels were reduced by 34.0 % ( $P < 0.05$  vs. HC), 26.3 % ( $P < 0.05$  vs. HC) and 45.6 % ( $P < 0.05$  vs. HC) in the cerebral artery, cerebral cortex and hippocampus, respectively. The ROS levels in vascular and brain tissues were basically consistent between the control group and the DXM and DXM+SL groups (Fig. 6).

### 3.6. eNOS and profibrotic factor expression in the cerebral artery

Compared to the control group, in the HC group, eNOS mRNA expression in the cerebral artery declined by 62.1 % compared ( $P < 0.05$ ). However, compared to the HC group, in the HC+SL group, eNOS mRNA levels were partly improved and increased by 75.2 % ( $P < 0.05$  vs. HC). eNOS expression was similar between the control group and the DXM and DXM+SL groups. The fold-changes in mRNA levels observed among the groups are expressed in a heat map in Fig. 7, and the mRNAs with significant differences are listed in Fig. 8.

Compared to the control group, in the HC group, the expression levels of the profibrotic factors  $\alpha$ -SMA and type 1 collagen were 1.52 and 1.73 times higher ( $P < 0.05$ ); however, compared to the HC group, in the HC+SL group, they were 61.2 % and 53.8 % lower, respectively ( $P < 0.05$  vs. HC). In the DXM and DXM+SL groups, the  $\alpha$ -SMA and type 1 collagen expression levels were almost identical to those observed in the HC group (Figs. 7, 8, Supplemental Fig. 3).

### 3.7. Proinflammatory factors and nNOS mRNA expression

In this study, we chose the proinflammatory factors CCR2, CCL7, CCL8, CCL12, interleukin 6 (IL-6), IL-1 $\beta$ , and TNF- $\alpha$  to evaluate the chronic inflammatory state in animals with glucocorticoid excess. As shown in Figs. 7 and 8, compared to the control rats, the HC-treated rats presented 1) higher levels of IL-1 $\beta$  and CCL8 mRNA expression in cerebral cortical neurons; 2) higher levels of IL-6, CCR2, CCL8, and CCL12 expression in hippocampal neurons; and 3) higher levels of TNF- $\alpha$ , CCR2 and CCL12 expression in the cerebral artery. All of these HC-induced changes in the levels of proinflammatory factors in the cortex,

hippocampus and vasculature were mitigated in the HC + SL group, and the proinflammatory factor expression in the DXM and DXM + SL groups remained the same as that observed in the control group (Figs. 7, 8).

The mRNA expression level of nNOS in the cerebral cortex and hippocampus tissues was 2.68-fold and 1.15-fold higher, respectively, in the HC group than in the control group but 41.3 % lower in the cerebral cortex after SL intervention ( $P < 0.05$ ). The increased nNOS expression induced by HC treatment was not observed in the DXM and DXM+SL groups (Figs. 7, 8, Supplemental Figs. 4,5).

### 3.8. MR and GR target gene expression

The expression levels of MR and the MR target genes Sgk-1 and NHE-1 in the cortex, hippocampus and cerebral artery were significantly higher in the HC group but not the DXM group than in the control group. GR expression was mainly activated in the DXM and DXM + SL groups but was also slightly higher in the HC and HC + SL groups than in the control group.

## 4. Discussion

To our knowledge, this is the first study to explore the potential role of MR hyperactivity in cerebral lesions in animals with glucocorticoid excess. The major findings of this study are that chronically elevated circulating glucocorticoid levels may cause cerebral cortex and hippocampal atrophy and cerebral vascular wall thickening in rats, and effect that was partially reversed by blocking the activation of MR. The activation of MRs caused by increased serum glucocorticoid levels was associated with ROS overproduction and chronic inflammation in the brain, which led to increased levels of cerebrovascular endothelial cell apoptosis and endothelial dysfunction, vascular fibrosis, and cerebral cortex/hippocampus neural apoptosis.

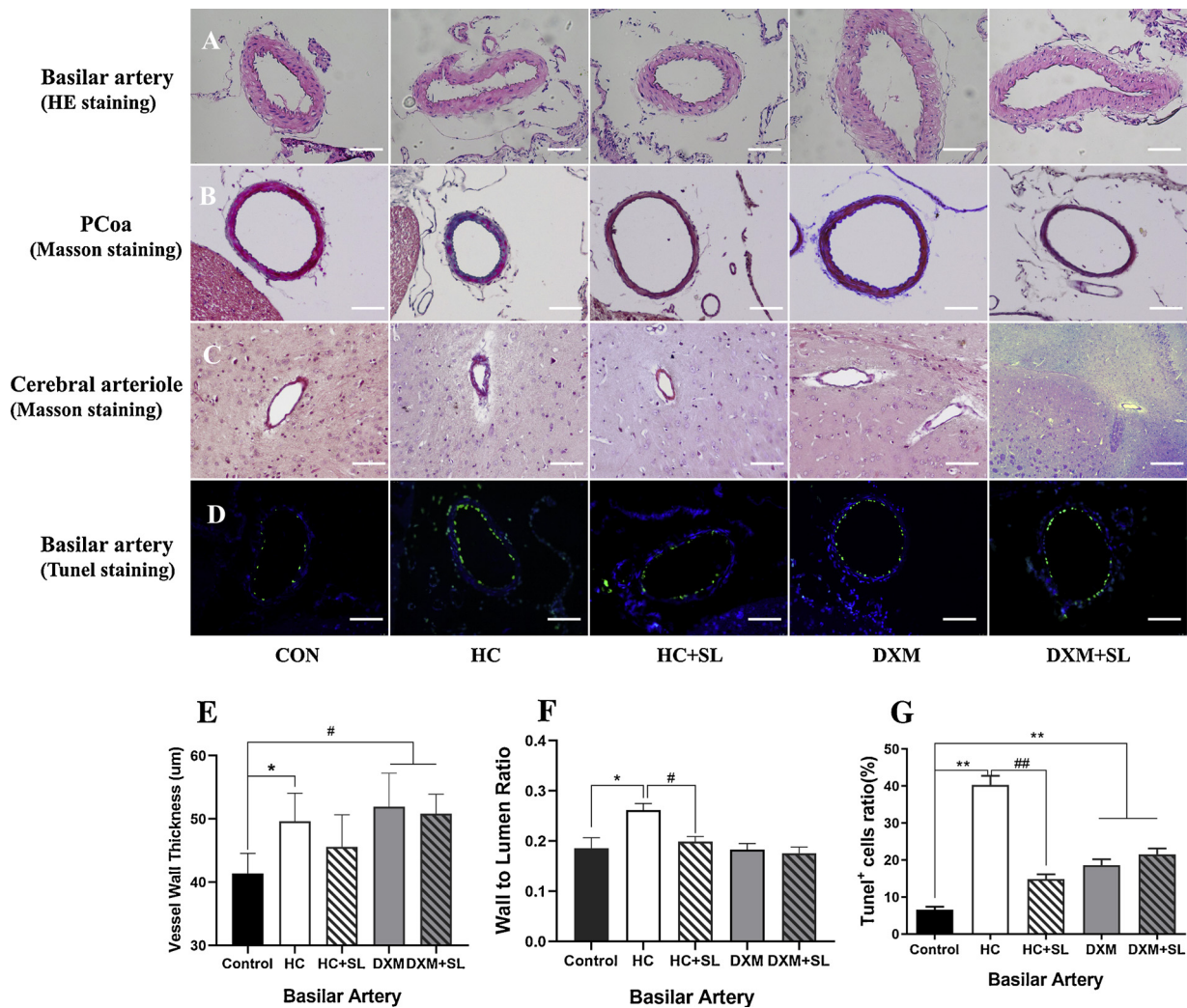


**Fig. 4.** Cerebrovascular morphology in different groups (magnification: A, B, C, D: ×200).

Basilar artery demonstrated increased wall thickness and a higher wall/lumen area ratio than control in HC rats by HE staining, of which both can be partially reversed by spironolactone. While DXM and DXM + SL group had equally thickened artery wall and unchanged wall/lumen area ratio compared with the control (A, E, F). PCoA and arterioles among the cortex by Masson's trichrome staining showed a collagen increase under HC treatment, while the HC + SL group had less fibrotic area than the HC group. DXM and DXM + SL groups also showed increased collagen (B, C). Quantification of apoptotic cells by the TUNEL assay was significantly increased following HC treatment and can be reversed by spironolactone. DXM and DXM + SL group also had equally increased apoptosis rate (D, G). The data are expressed as mean ± SEM, n = 6–8 for each experiment. \*P < 0.05 \*\*P < 0.01 vs Control. #P < 0.05 ##P < 0.01 vs HC group. PCoA: posterior communicating artery. Scale bars: 50 µm.

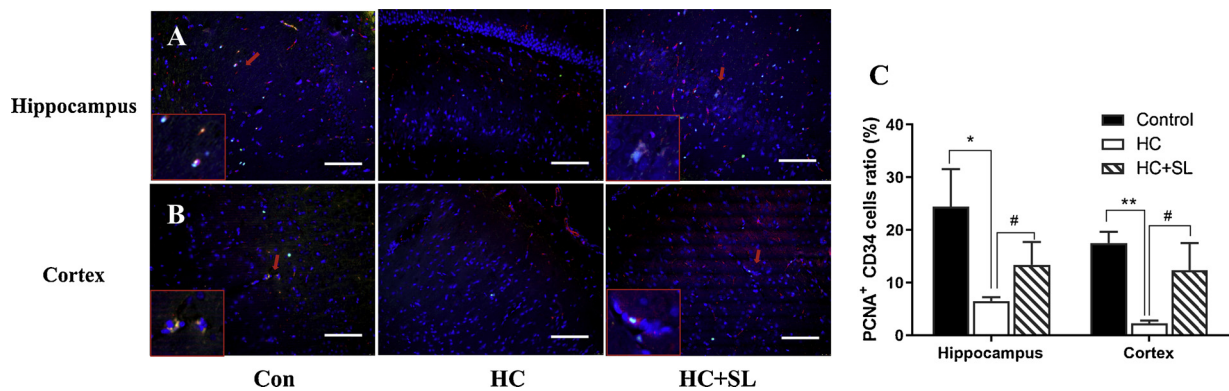


**Fig. 5.** Immunofluorescence proliferation in cerebral microvascular (magnification: A, B: ×200).

Double staining for PCNA (green) and CD34 (red) showed that decreased expression of proliferation in hippocampal(A) and cortical(B) neurons in the HC group. Representative examples of the areas were showed in red squares; The quantification of microvascular proliferation in the HC group was significantly inhibited and can be obviously improved by the administration of spironolactone (C). \*P < 0.05 \*\*P < 0.01 vs Control. #P < 0.05 ##P < 0.01 vs HC group. Values were expressed as mean ± SEM, n = 6. Scale bars: 50 µm.

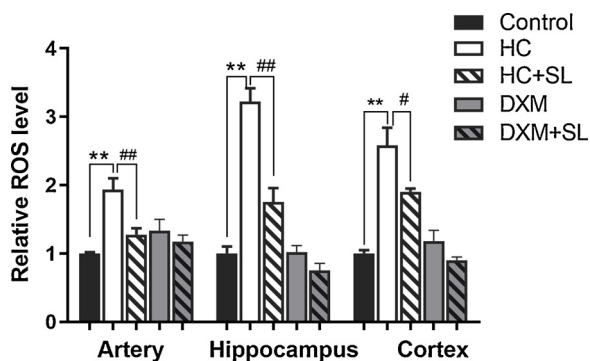


**Fig. 6.** ROS levels in the cerebral artery, cerebral cortex and hippocampus. \*P < 0.05 \*\*P < 0.01 vs Control. #P < 0.05 ##P < 0.01 vs HC group. Values were expressed as mean ± SEM, n = 6. ROS: reactive oxygen species.

**4.1. Hypercortisolemia-associated brain atrophy may contribute to MR hyperactivity in the cortex and hippocampus**

In this study, the brain to body weight ratio was lower in the HC group than in the control group, which suggests the possibility that brain atrophy occurs in HC-treated animals. Nissl staining with hypochromic cortical area identified injured neurons and HE staining confirmed that neuron numbers were lower, while the rate of neuronal apoptosis in dentate gyrus (which is the site of neuronal birth and apoptosis) was higher in the cortex and hippocampus in the HC group but not the DXM group than in the control group. We noticed that the mRNA expression levels of MR and the MR target genes Sgk-1 and NHE-1 in the cortex and hippocampus were significantly higher in the HC group but not in DXM group than in the control group, while GR expression was activated in both the DXM and HC groups. In view of the low affinity between DXM and MR, we believe that the brain damage related to chronic glucocorticoid exposure might be mainly mediated by enhanced MR activity. The brain morphological changes observed in HC-treated rats were partially alleviated when SL was used to block MR, further confirming the important role of MR activation in glucocorticoid-related brain injury. Since cerebral 11bHSD2 gene expression were not altered and 11bHSD2 gene expression was almost undetectable in the cortex and the hippocampus in HC group and thus losing its protective role, it is logical to speculate that elevated glucocorticoid concentrations are capable of leading to MR overactivation in the cortex and hippocampus.

It was previously demonstrated that aldosterone-treated rats exhibit progressive renal injury and that this effect was suppressed by an MR

antagonist [24]. Rafiq et al. reported that eplerenone attenuated hydrocortisone-induced but not DXM-induced renal injury without affecting blood pressure [10]. Our study is the first to verify that similar changes occur in brain tissues. We found that the levels of UACR and brain injury were higher in HC-treated animals than in controls and that these effects could be partially mitigated by MR antagonists. It is therefore reasonable to speculate that the brain atrophy associated with glucocorticoid excess may contribute to MR activation.

**4.2. Cerebrovascular injury caused by MR and GR overactivation is also involved in the development of hyperglucocorticoidemia-associated brain atrophy**

We compared the histological changes that occurred in cerebral vessels in different treatment groups. Compared with the control group, in the HC group, the cerebral vasculature of the rats showed a higher wall thickness, higher wall/lumen areas, a higher rate of endothelial cell apoptosis, a larger fibrotic area (PCoA), and a lower rate of microvascular proliferation in the hippocampus and cortex. In addition, compared to the control group, the HC-treated animals had higher levels of MR and MR target genes in the cerebral artery, indicating enhanced MR activity, and SL intervention decreased the HC-induced changes in MR target gene expression and partially alleviated HC-induced vascular damage. These results indicate that MR hyperactivity may be involved in the pathological process in which vascular injury is associated with chronic glucocorticoid exposure.

Over the past decade, it has become clear that MR is expressed in the cardiovascular system, and the presence of functional MRs in vascular smooth muscle and endothelial cells has been well established [9,14]. Human data, in vivo animal studies and in vitro studies have suggested that MR activation plays a role in promoting vessel fibrosis and remodeling [25]. The results of our study are consistent with these previous findings. Compared with the control group, the HC-treated animals had higher levels of the fibrotic markers a-SMA and type 1 collagen, whereas DXM treatment did not exert these effects. a-SMA is a skeletal protein expressed in vascular smooth muscle and a marker protein of the vascular smooth muscle contractile phenotype [26], while T1C plays an important role in maintaining vascular integrity [27]. The higher levels of a-SMA and T1C observed in the HC group suggest an increase in vascular wall fibrosis and abnormal morphology, and HE and Masson staining showed stenosis of the lumen and thickening of the vessel wall in rats in this group. As the MR blocker SL partially abolished these increases, we conclude that MR activation might mediate excess glucocorticoid-induced cerebrovascular injury. Since cerebral 11bHSD1 and 11bHSD2 gene expression was not altered

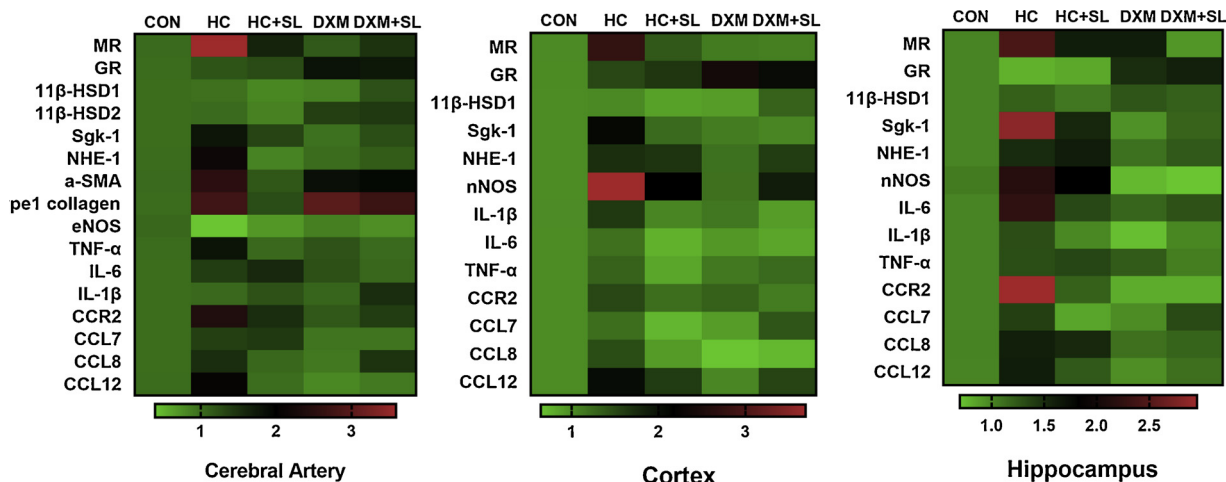


**Fig. 7.** Heat map of mRNA fold change in each group. Gene mRNA expression in the cerebral artery, cortex and hippocampus. Values were expressed as mean ± SEM, n = 6.

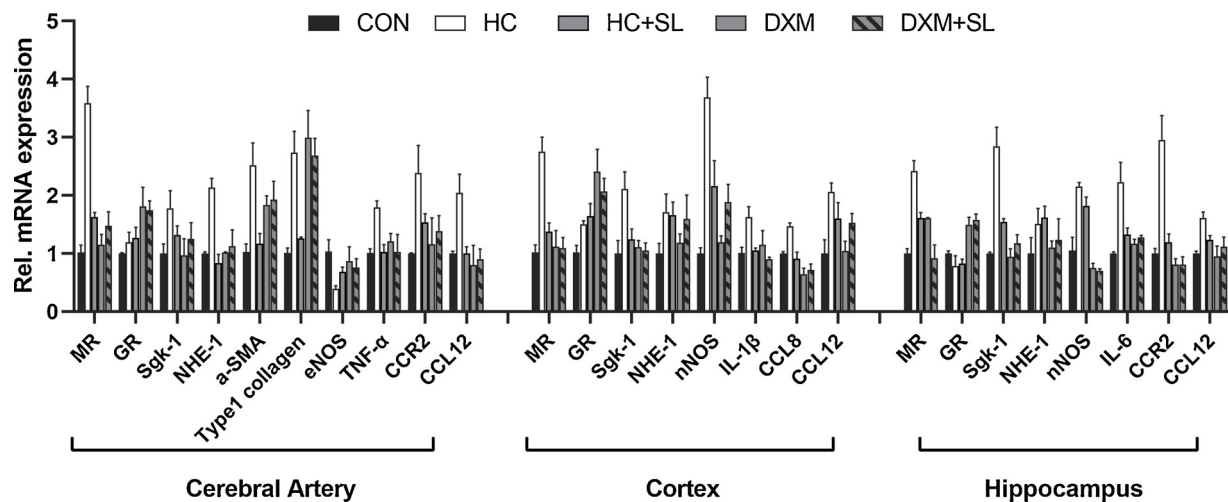


Fig. 8. mRNAs with significant differences in each group.

Gene mRNA expression in the cerebral artery, cortex and hippocampus. Values were expressed as mean  $\pm$  SEM,  $n = 6$ .

in the vessels, it is logical to speculate that elevated glucocorticoid concentrations are capable of overcoming the protective role of 11 $\beta$ HSD2, leading to MR overactivation in the cerebral vasculature.

A similar but slight change in vascular morphology also occurred in the rats in the DXM group, and SL did not improve these DXM-related vascular injuries, suggesting that GR activation was also involved in the vascular damage caused by glucocorticoids [25,28]. Brain atrophy is related to cerebrovascular disease [29]. The increased vascular wall thickness and decreased lumen area observed in glucocorticoid-treated rats may lead to ischemia and hypoxia of brain tissues, thus inducing cerebral cell loss. We believe that cerebrovascular injury might also play an important role in the development of brain atrophy caused by chronic glucocorticoid excess.

#### 4.3. Increased ROS production and the chronic inflammation due to MR activation may be a potential pathophysiological mechanism underlying glucocorticoid-related brain atrophy

A proinflammatory role for MR has been demonstrated in animal models of atherosclerosis [30,31]. Furthermore, elevated systemic aldosterone levels were shown to cause oxidative stress and endothelial dysfunction in the cerebral circulation [17,32,33]. It has also been demonstrated that MRs are highly expressed in many brain regions, including cerebral vessels [16,34]. Consistent with this finding, our results showed that in the cerebral artery, cerebral cortex and hippocampus, MR and MR target gene expression was enhanced in HC-treated animals and that the ROS levels, the levels of proinflammatory factors and the nNOS mRNA expression levels observed in these animals corresponded to increased ROS levels. Given that the MR antagonist SL can decrease oxidative stress and inflammatory marker expression and that these changes were not observed in the DXM-treated animals in this study, we believe that the increased oxidative stress and inflammation that were associated with excessive MR activity in this study represent pathophysiological connections between brain atrophy and prolonged exposure to excess glucocorticoids.

In this study, we used HC but not corticosterone (a primary circulating glucocorticoid in rats) to model Cushing's syndrome in humans. Because many studies have reported that HC also has glucocorticoid activity in rats [35,36], we believe that HC administration creates an excess glucocorticoid exposure state. In addition, we did not use a specific GR antagonist to examine the involvement of GR activation in rats. DXM is a glucocorticoid agonist with no apparent MR agonistic activity. DXM administration increased cerebrovascular wall thickness and cellular apoptosis accompanied by elevated profibrotic expression,

which cannot be alleviated by SL treatment, suggesting that GR activation was also involved in the vascular damage. However, no morphological or proinflammatory gene changes were observed in DXM-treated cortex or hippocampus. In the previous studies, exposure to higher concentration of DXM was proven to have pro-inflammatory effects in the brain and cause neurodegeneration in developing rat brains [37,38]. Contrary to toxic effects, DXM can reduce ischemia-induced cerebral apoptotic death and superoxide anion production in the brain [39–41]. Timing, concentration, and duration of DXM exposure are critical in determining to be whether neurotrophic or neuroprotective. The GR knockdown [42] or overexpression [43] mouse models were often used in the psychopathology of depression and stress response. The GR in cardiovascular system had been deeply investigated [44] but no study had explored the relationship between GR and cerebrovascular system. Taken together with our present findings and the complex crosstalk between GR and MR, we could not eliminate the possibility that the changes in the brain and cerebral artery were partly GR-dependent responses. Future basic research must be made to clarify the GR or MR role on different cell types and brain regions.

## 5. Conclusion

In this study, we provide the first confirmation that chronically elevated circulating glucocorticoid concentrations may enhance oxidative stress and inflammation in rat cerebral vessels and brain tissue via a MR activation-mediated mechanism. Our results suggest that MR activation in the hyperglucocorticoidemia state contributes to cerebrovascular fibrosis and remodeling and thereby promotes neural apoptosis in the cerebral cortex/hippocampus. Further exploration of the molecular mechanisms underlying the detrimental effects of excess glucocorticoids on the brain could lead to the identification of novel therapeutic targets to prevent or treat nervous system complications and cardiovascular disorders.

### Data availability statement

All data are available upon request.

### Ethics statement

This study had been approved by the Institutional Animal Care and Use Committee of The West China Hospital.

## Author contributions

Yaxi Chen, Jingtao Qiao, Leilei Zhu and Zhen Xiao conducted the experiments. Yaxi Chen and Jingtao Qiao performed the analysis. Yaxi Chen and Yerong Yu designed the experiments and wrote the paper.

## Declaration of Competing Interest

No potential conflicts of interest relevant to this article were reported.

## Appendix A. Supplementary data

Supplementary material related to this article can be found, in the online version, at doi:<https://doi.org/10.1016/j.biopha.2019.109695>.

## References

- [1] E. Resmini, A. Santos, S.M. Webb, Cortisol excess and the brain, *Front. Horm. Res.* 46 (2016) 74–86.
- [2] M.I. Schubert, et al., Effects of altered corticosteroid milieu on rat hippocampal neurochemistry and structure—an in vivo magnetic resonance spectroscopy and imaging study, *J. Psychiatr. Res.* 42 (11) (2008) 902–912.
- [3] J.J. Cerqueira, et al., Corticosteroid status influences the volume of the rat cingulate cortex - a magnetic resonance imaging study, *J. Psychiatr. Res.* 39 (5) (2005) 451–460.
- [4] A. Mahfouz, et al., Genome-wide coexpression of steroid receptors in the mouse brain: identifying signaling pathways and functionally coordinated regions, *Proc Natl Acad Sci U S A* 113 (10) (2016) 2738–2743.
- [5] J.W. Funder, Mineralocorticoid receptors: distribution and activation, *Heart Fail. Rev.* 10 (1) (2005) 15–22.
- [6] M.E. Baker, J.W. Funder, S.R. Kattoula, Evolution of hormone selectivity in glucocorticoid and mineralocorticoid receptors, *J. Steroid Biochem. Mol. Biol.* 137 (2013) 57–70.
- [7] E.P. Gomez-Sanchez, Mineralocorticoid receptors in the brain and cardiovascular regulation: minority rule? *Trends Endocrinol. Metab.* 22 (5) (2011) 179–187.
- [8] M. Nagase, T. Fujita, Endocrinological aspects of proteinuria and podocytopathy in diabetes: role of the aldosterone/mineralocorticoid receptor system, *Curr. Diabetes Rev.* 7 (1) (2011) 8–16.
- [9] P. Wilson, et al., Mediators of mineralocorticoid receptor-induced profibrotic inflammatory responses in the heart, *Clin. Sci.* 116 (9) (2009) 731–739.
- [10] K. Rafiq, et al., Effects of mineralocorticoid receptor blockade on glucocorticoid-induced renal injury in adrenalectomized rats, *J. Hypertens.* 29 (2) (2011) 290–298.
- [11] C.S. Wyrwoll, M.C. Holmes, J.R. Seckl, 11 $\beta$ -hydroxysteroid dehydrogenases and the brain: from zero to hero, a decade of progress, *Front. Neuroendocrinol.* 32 (3) (2011) 265–286.
- [12] C. Sabbadin, D. Armanini, Syndromes that mimic an excess of mineralocorticoids, *High Blood Press. Cardiovasc. Prev.* 23 (3) (2016) 231–235.
- [13] G.P. Vyssoulis, et al., Aldosterone levels and stroke incidence in essential hypertensive patients, *Int. J. Cardiol.* 144 (1) (2010) 171–172.
- [14] A.J. Rickard, et al., Endothelial cell mineralocorticoid receptors regulate deoxycorticosterone/salt-mediated cardiac remodeling and vascular reactivity but not blood pressure, *Hypertension* 63 (5) (2014) 1033–1040.
- [15] A. Buglioni, et al., Circulating aldosterone and natriuretic peptides in the general community: relationship to cardiorenal and metabolic disease, *Hypertension* 65 (1) (2015) 45–53.
- [16] C.S. Rigsby, et al., Intact female stroke-prone hypertensive rats lack responsiveness to mineralocorticoid receptor antagonists, *Am. J. Physiol. Regul. Integr. Comp. Physiol.* 293 (4) (2007) R1754–63.
- [17] S. Chrissobolis, et al., Chronic aldosterone administration causes Nox2-mediated increases in reactive oxygen species production and endothelial dysfunction in the cerebral circulation, *J. Hypertens.* 32 (9) (2014) 1815–1821.
- [18] O. Thellin, et al., A decade of improvements in quantification of gene expression and internal standard selection, *Biotechnol. Adv.* 27 (4) (2009) 323–333.
- [19] D.E. Korzhevskii, V.A. Otellin, Immunocytochemical demonstration of astrocytes in brain sections combined with Nissl staining, *Morfologija* 125 (3) (2004) 100–102.
- [20] T. Ito, Y. Nishimura, J. Saavedra, Pre-treatment with candesartan protects from cerebral ischaemia, *J. Renin. Syst.* 2 (3) (2001) 174–179.
- [21] D.Y. Mason, K. Micklem, M. Jones, Double immunofluorescence labelling of routinely processed paraffin sections, *J. Pathol.* 191 (4) (2000) 452–461.
- [22] E.A. Renzoni, et al., Interstitial vascularity in fibrosing alveolitis, *Am. J. Respir. Crit. Care Med.* 167 (3) (2003) 438–443.
- [23] P. Ma, et al., Intraperitoneal injection of magnetic Fe<sub>3</sub>O<sub>4</sub>-nanoparticle induces hepatic and renal tissue injury via oxidative stress in mice, *Int. J. Nanomedicine* 7 (2012) 4809–4818.
- [24] H. Kiyomoto, et al., Possible underlying mechanisms responsible for aldosterone and mineralocorticoid receptor-dependent renal injury, *J. Pharmacol. Sci.* 108 (4) (2008) 399–405.
- [25] A. McCurley, I.Z. Jaffe, Mineralocorticoid receptors in vascular function and disease, *Mol. Cell. Endocrinol.* 350 (2) (2012) 256–265.
- [26] H. Shen, et al., Activation of TGF- $\beta$ 1/ $\alpha$ -SMA/Col I profibrotic pathway in fibroblasts by Galectin-3 contributes to atrial fibrosis in experimental models and patients, *Cell. Physiol. Biochem.* 47 (2) (2018) 851–863.
- [27] G. Bou-Gharios, et al., Extra-cellular matrix in vascular networks, *Cell Prolif.* 37 (3) (2004) 207–220.
- [28] J.E. Goodwin, et al., Knockout of the vascular endothelial glucocorticoid receptor abrogates dexamethasone-induced hypertension, *J. Hypertens.* 29 (7) (2011) 1347–1356.
- [29] A. Nitkunan, et al., Brain atrophy and cerebral small vessel disease: a prospective follow-up study, *Stroke* 42 (1) (2011) 133–138.
- [30] J. Suzuki, et al., Eplerenone with valsartan effectively reduces atherosclerotic lesion by attenuation of oxidative stress and inflammation, *Arterioscler. Thromb. Vasc. Biol.* 26 (4) (2006) 917–921.
- [31] S. Keidar, et al., Aldosterone administration to mice stimulates macrophage NADPH oxidase and increases atherosclerosis development: a possible role for angiotensin-converting enzyme and the receptors for angiotensin II and aldosterone, *Circulation* 109 (18) (2004) 2213–2220.
- [32] Q.N. Dinh, et al., Aldosterone-induced oxidative stress and inflammation in the brain are mediated by the endothelial cell mineralocorticoid receptor, *Brain Res.* 1637 (2016) 146–153.
- [33] D.A.B. Kasal, et al., T regulatory lymphocytes prevent aldosterone-induced vascular injury, *Hypertension* 59 (2) (2012) 324–330.
- [34] Q.N. Dinh, et al., Aldosterone and the mineralocorticoid receptor in the cerebral circulation and stroke, *Exp. Transl. Stroke Med.* 4 (1) (2012) 21.
- [35] P.P. Nunes, et al., Chronic low-dose glucocorticoid treatment increases subcutaneous abdominal fat, but not visceral fat, of male Wistar rats, *Life Sci.* 190 (2017) 29–35 (undefined).
- [36] Y. Feng, et al., Dexamethasone but not the equivalent doses of hydrocortisone induces neurotoxicity in neonatal rat brain, *Pediatr. Res.* 77 (5) (2015) 618–624.
- [37] Y. Feng, et al., Dexamethasone induces neurodegeneration but also up-regulates vascular endothelial growth factor A in neonatal rat brains, *Neuroscience* 158 (2) (2009) 823–832.
- [38] C.R. Neal, et al., Effect of neonatal dexamethasone exposure on growth and neurological development in the adult rat, *Am. J. Physiol. Regul. Integr. Comp. Physiol.* 287 (2) (2004) R375–85.
- [39] J.D. Barks, M. Post, U.I. Tuor, Dexamethasone prevents hypoxic-ischemic brain damage in the neonatal rat, *Pediatr. Res.* 29 (6) (1991) 558–563.
- [40] A.M. Gorman, et al., Dexamethasone pre-treatment interferes with apoptotic death in glioma cells, *Neuroscience* 96 (2) (2000) 417–425.
- [41] C.A. Colton, O.N. Chernyshev, Inhibition of microglial superoxide anion production by isoproterenol and dexamethasone, *Neurochem. Int.* 29 (1) (1996) 43–53.
- [42] D. Matrov, et al., Cerebral oxidative metabolism mapping in four genetic mouse models of anxiety and mood disorders, *Behav. Brain Res.* 356 (2019) 435–443 (undefined).
- [43] Q. Wei, et al., Glucocorticoid receptor overexpression in forebrain: a mouse model of increased emotional lability, *Proc. Natl. Acad. Sci. U. S. A.* 101 (32) (2004) 11851–11856.
- [44] B. Liu, et al., The glucocorticoid receptor in cardiovascular health and disease, *Cells* 8 (10) (2019).